

# Statement of Research Interests

Michael Strickland

## 1 Research Summary

The beginning of experiments at the Relativistic Heavy-Ion Collider (RHIC) at Brookhaven National Laboratory in 1999 marked the beginning of a new era in ultrarelativistic heavy-ion collisions. One of the primary goals of the RHIC program is to discover and study the quark-gluon plasma (QGP) whose existence is predicted by quantum chromodynamics (QCD). In addition, ultrarelativistic heavy-ion collision experiments are part of the Large Hadron Collider (LHC) program at CERN. The LHC experiments, for which full beam runs are scheduled in 2008, will provide data on heavy ion collisions at center of mass energies of 5.5 TeV and will open a new chapter in the study of partonic matter under extreme conditions. For the RHIC and LHC experiments to have the greatest possible impact on science, it is essential to make as close a connection to fundamental theory as possible. Currently, however, there is a large gulf between the fundamental theory of the quark-gluon plasma derived from quantum chromodynamics (QCD) and the phenomenology of heavy-ion collisions. There is an urgent need for theoretical analysis that is based rigorously on QCD but which can also make contact with more phenomenological approaches.

I am pursuing this goal on multiple fronts. Most recently, I have been working together with collaborators to calculate the effects of having anisotropic quark and gluon momentum-space distribution functions on the isotropization, thermalization, and signatures of a quark-gluon plasma. This endeavor is probing the frontiers of non-equilibrium gauge field theory. Recently, in particular, we have been able to describe the appearance of the experimentally observed “ridge” in the rapidity-azimuthal plane as coming from deflection of the jet by medium chromofields (see Sec. 2.1). Another major effort I am pursuing is the development of a new perturbative approach to thermal QCD, dubbed hard-thermal-loop perturbation theory (HTLpt), in which plasma effects are built in at leading order instead of being taken into account through higher order corrections. The goal of this line of research is to develop this new approach into a reliable phenomenological tool for studying signatures for the quark-gluon plasma in heavy-ion collisions which does not suffer from the convergence problems of naively resummed perturbation theory.

## 2 Non-equilibrium Gauge Theories – Observables

In the last four years I have focused my efforts on finding a framework for determining the effects of early-time non-equilibrium physics on heavy-ion observables including QGP jet energy loss and  $p_T$ -broadening, and electromagnetic signatures. We have found in the process that the rapid longitudinal expansion of the quark-gluon plasma induces unstable modes in the plasma. These unstable modes cause a rapid transfer of energy from hard to soft scales where the energy is deposited initially as *coherent color fields*. In a non-Abelian plasma this coherence is replaced at late times by a *turbulent cascade* of energy from large to small scales (see Fig. 5 right). This cascade generates a saturated large-amplitude turbulent field background through which the partons must traverse.

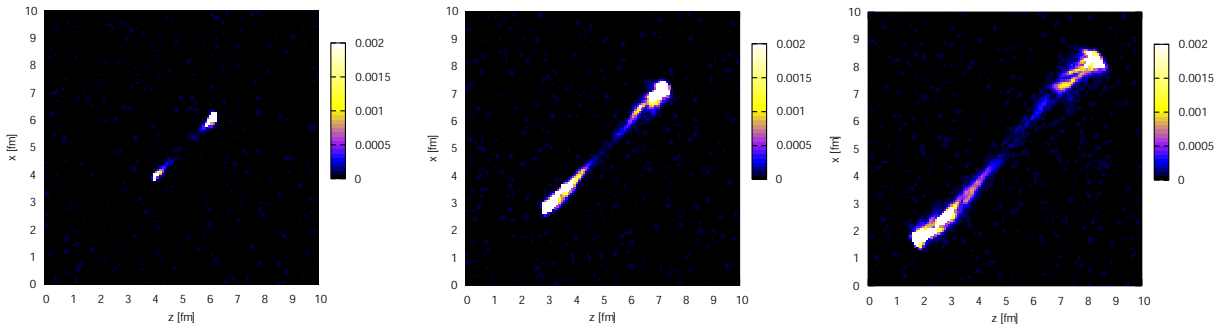


Figure 1: Snapshots of a particle-antiparticle jet (directed along diagonal) propagating through a quark-gluon plasma particle-in-cell (PIC) simulation which includes the effects of collisions and chromofield dynamics. Coloration shows the intensity of the local chromo-magnetic fields induced by the passage of the jet through the medium. This intensity provides a measure of where and when energy is deposited in the plasma due to jet traversal.

Both the large-amplitude coherent phase and subsequent turbulent “glasma” can have a significant effect on particle dynamics resulting in, among other things, longitudinal pressure which drives the system toward isotropy. With our new understanding of this “chromo-Weibel” instability it is now possible to calculate the effect of expansion induced momentum-space anisotropies on QGP observables. The general techniques used include both analytical calculations and numerical simulations. Below I review my recent work in these areas.

## 2.1 Realtime Jet Dynamics with Colored Particle-in-Cell (CPIC) Simulations

One avenue which my collaborators and I have been pursuing is numerical solution of the realtime QCD Boltzmann-Vlasov equations on large ( $64^3$  and  $128^3$ ) three-dimensional lattices. These codes are similar to standard PIC (particle-in-cell) codes which are used to simulate electromagnetic plasmas but extend the approach to particles with non-Abelian charge and fields with non-Abelian self-interactions. Particles are represented as  $N_{\text{test}}$  “test” particles and as these test particles “fly” around the lattice they are deflected and color-rotated by the dynamically evolving chromoelectromagnetic fields. In practice, the code evolves the particle positions (currents), chromoelectric field, and gauge link plaquette variables which are a gauge-invariant representation of the chromomagnetic field. In addition, we include binary collisions between the test particles with the frequency and angular distribution set by the leading order perturbative QCD collisional cross section. In practice the collision probability distribution is used and collisions are sampled from this distribution using the so-called stochastic method. In this way, we are able to produce *ab initio* calculations of real-time transport properties of a quark-gluon plasma including field-field, particle-field, and particle-particle interactions.

In Fig. 1 I show a visualization of a hard-gluon jet propagating through a self-consistently generated in-medium background field distribution. The coloration indicates the intensity of the chromomagnetic fields induced by the jet’s passage through the medium. With simulations like this we are able to study in detail the question of collective effects on high-energy jet propagation. In our most recent work [1] we have studied the momentum-space diffusion of high-energy jets in the presence the chromo-Weibel instability and have shown that the action of the instability is to preferentially broaden jets more along the rapidity direction than the azimuthal direction. This is due to the fact that the chromo-Weibel instability has on average  $E_L^2 > E_T^2$  and  $B_T^2 > E_T^2$  during

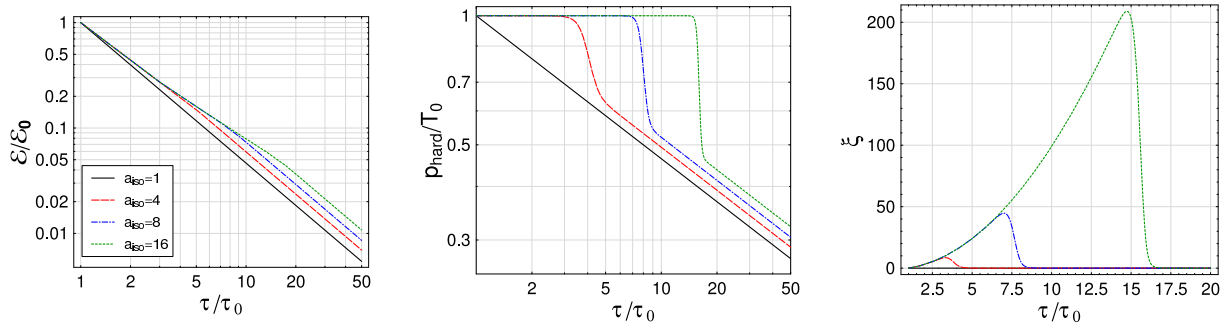


Figure 2: Model energy density (left), hard momentum scale (middle), and anisotropy parameter (right) for four different isotropization times  $\tau_{\text{iso}} \in \{0.1, 0.4, 0.8, 1.6\}$  fm/c assuming  $\tau_0 = 0.1$  fm/c and  $\gamma = 2$ .

the period of time when the instability is growing. This preferential broadening of the jet could possibly explain the observed “ridge” see in STAR near-side jet analysis (two particle correlations).

## 2.2 Non-equilibrium effects on QGP electromagnetic observables

One major defect of the canonical analyses of QGP in-medium particle production is that they have traditionally assumed that the plasma is generated in an isotropic thermal state. This assumption is particularly strong in the calculation of electromagnetic observables where the standard analyses typically assume that the plasma is thermal and isotropic already at the parton formation time ( $\tau_{\text{iso}} = \tau_0 \sim 0.1\text{-}0.3$  fm/c). As with any assumption one must test the consequences of relaxing it on experimental observables.

Absent a precise dynamical picture of the first few fm/c of the QGP’s lifetime I have recently [2] proposed a simple phenomenological model for the time-dependence of the plasma momentum-space anisotropy,  $\xi = \langle p_T^2 \rangle / \langle p_L^2 \rangle - 1$ , and hard momentum scale,  $p_{\text{hard}}$ . I then use this model to explore the effect of early-time plasma momentum-space anisotropies on high-energy dilepton production. To accomplish this I introduce two parameters: (1)  $\tau_{\text{iso}}$  which is the proper time at which the system begins behaving hydrodynamically and (2)  $\gamma$  which sets the sharpness of the transition to hydrodynamic behavior. For times greater than the parton formation time,  $\tau_0$ , but short compared to  $\tau_{\text{iso}}$  I assume that the system is free streaming and for times long compared to  $\tau_{\text{iso}}$  that it is expanding hydrodynamically. A typical time evolution of the model energy density, hard scale, and anisotropy parameter  $\xi$  are shown in Fig. 2.

In Fig. 3 I show my recently published results for the resulting dilepton spectra as a function of both transverse momentum (left),  $p_T$ , and pair invariant mass (right),  $M$ , compared to other background sources. As can be seen from Fig. 3 there is a significant variation of the medium dilepton yield when varying the assumed plasma isotropization time,  $\tau_{\text{iso}}$ , from 0.088 fm/c to 2 fm/c. As a function of invariant mass when an isotropization time of 2 fm/c is assumed we see that medium dileptons become as important as Drell-Yan and jet conversion. The reason for the enhanced production is that free streaming preserves more transverse momentum than an isotropically expanding plasma.

As I show in Fig. 3 (left) as a function of  $p_T$  the medium contribution dominates the expected Drell-Yan and jet conversion sources for all  $p_T < 6$  GeV. If an isotropization time of 2 fm/c is assumed then the medium dileptons dominate out to  $p_T \sim 9$  GeV. This dominance means that it

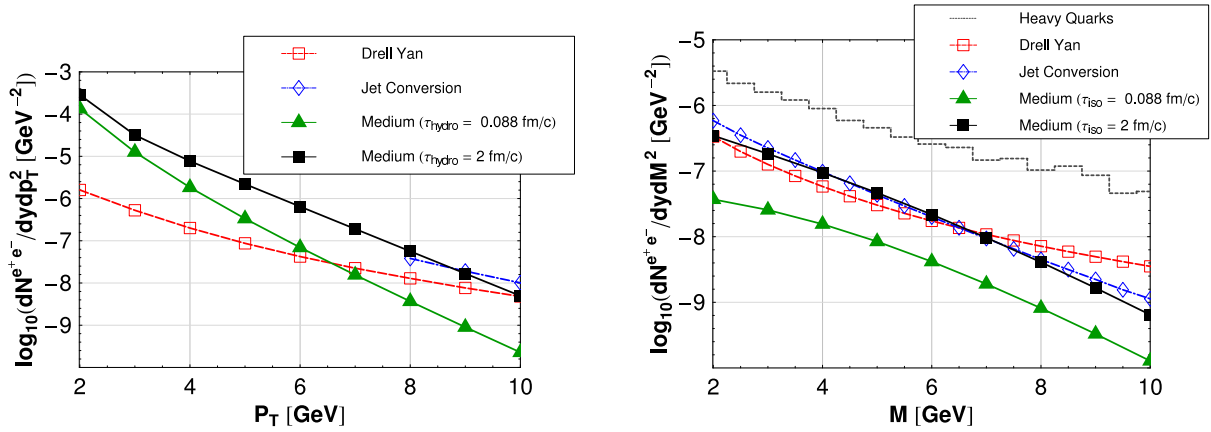


Figure 3: Dilepton yields as a function of (a) transverse momentum with a cut  $0.5 < M < 1$  GeV and (b) invariant mass with a cut  $p_T > 8$  GeV. For medium dileptons we use  $\gamma = 2$  and  $\tau_{\text{iso}}$  is taken to be either 0.088 fm/c or 2 fm/c.

should be possible to use dilepton production to determine much-needed information about quark-gluon plasma initial conditions at LHC. As can be seen from Fig. 3 at  $p_T = 5$  GeV the expected medium dilepton yield varies by nearly an order of magnitude depending on the assumed plasma isotropization time.

Based on Fig. 3 it should be possible to measure  $\tau_{\text{iso}}$  at LHC energies using dilepton production in the kinematic range  $3 < p_T < 8$  GeV. Additionally via my model for  $\xi(\tau)$  shown in Fig. 2 determining  $\tau_{\text{iso}}$  provides an estimate of the maximum amount of momentum-space anisotropy achieved during the lifetime of the QGP. Together with my PhD students I am currently extending the calculation of the in-medium anisotropic dilepton to next-to-leading order. We are also applying the same space-time model to photons and other observables in order to assess the effect of possible early-time momentum-space anisotropies on these observables. For medium photon production a similar production enhancement is observed when a QGP thermalization time,  $\tau_{\text{iso}} \sim 1$  fm/c is assumed.

### 3 Non-equilibrium Gauge Theories and QGP Thermalization

One of the puzzles emerging from the RHIC ultrarelativistic heavy-ion collision experiments is that some observables like collective flow and soft-particle spectra are well-described by ideal hydrodynamic models which assume a very small plasma thermalization time  $\tau_{\text{iso}} < 1$  fm/c. In order to apply ideal hydrodynamical models the chief requirement is that the stress-energy tensor be isotropic in momentum space since having a local momentum-space anisotropy requires (at the very least) the inclusion of shear viscosity. Additionally, current ideal hydrodynamic treatments also assume that they can use an equilibrium equation of state to describe the time evolution of the produced matter. Therefore, the success of these models suggests that the bulk matter produced is *isotropic* and *thermal* at very early times,  $t < 1$  fm/c. Estimates of the isotropization and thermalization times from early perturbative calculations [4], however, indicated that the time scale for thermalization is more on the order of  $t \sim 2 - 3$  fm/c. This contradiction has led some to conclude that perturbation theory should be abandoned and replaced by a large strong coupling constant calculational framework. However, it has been proven recently that the early calculations of the isotropization and equilibration times had overlooked an important aspect of nonequilibrium

gauge field dynamics, namely the possibility of *plasma instabilities*.

These plasma instabilities cause the early stage QGP to have non-perturbative occupation numbers for soft fields<sup>1</sup> similar to what occurs in the saturated color-glass-condensate initial conditions for URHIC collisions. These non-perturbatively large field amplitudes ( $f \sim 1/\alpha_s$ ) mean that even at small values of the strong coupling constant ( $\alpha_s \sim 0.2 - 0.3$ ) the system can be **strongly-coupled** due to strong particle-field and field-field interactions. The possibility of generating strongly-coupled systems in a theory which doesn't necessarily have a strong coupling constant is familiar from studies of conventional QED plasmas where, of course, the electromagnetic coupling is very small,  $\alpha_s \sim 1/137$ , and still the system can be strongly-coupled via plasma collective modes.

A priori it is not even clear that the matter produced in an ultrarelativistic heavy-ion collision will thermalize at all. One of the chief obstacles to thermalization in such collisions is the intrinsic expansion of the matter produced. If the matter expands too quickly then there will not be time enough for its constituents to interact before flying apart into non-interacting particles and therefore the system will not reach thermal equilibrium. In a heavy-ion collision the expansion which is most relevant is the longitudinal (along the beamline) expansion of the matter since at early times it's much larger than the radial expansion. In the absence of interactions the longitudinal expansion causes the system to quickly become much colder in the longitudinal direction than in the transverse (radial) direction,  $\langle p_L^2 \rangle \ll \langle p_T^2 \rangle$ . We can then ask how long it would take for interactions to restore isotropy in the  $p_T$ - $p_L$  plane. In the bottom-up scenario [4] isotropy is obtained by hard collisions between the high-momentum modes which interact via an isotropically screened gauge interaction. The bottom-up scenario assumed that the underlying soft gauge modes responsible for the screening were the same in an anisotropic plasma as in an isotropic one. In fact, this turns out to be incorrect and in anisotropic plasmas the most important collective mode corresponds to an instability to transverse magnetic field fluctuations [5]. Recent works have shown that the presence of these instabilities is generic for distributions which possess a momentum-space anisotropy [6, 7] and have obtained the full hard-loop action in the presence of an anisotropy [8].

In the last year there have been significant advances made by using numerical solution of the full hard-loop effective action on real-time lattices. The purpose of these studies is to address the question of the long-time behavior of the instability evolution [9, 10, 11, 12]. This question is non-trivial in QCD due to the presence of non-linear interactions between the gauge degrees of freedom. These non-linear interactions become important when the vector potential amplitudes become  $\langle A \rangle_{\text{soft}} \sim p_{\text{soft}}/g \sim (gp_{\text{hard}})/g$ , where  $p_{\text{hard}}$  is the characteristic momentum of the hard particles. In QED there is no such complication and the fields grow exponentially until  $\langle A \rangle_{\text{hard}} \sim p_{\text{hard}}/g$  at which point the hard particles undergo large-angle scattering in the soft background field invalidating the assumptions underpinning the hard-loop effective action. Initial numerical toy models indicated that non-abelian theories in the presence of instabilities would “abelianize” and fields would saturate at  $\langle A \rangle_{\text{hard}}$  [9]. This picture was largely confirmed by simulations of the full hard-loop gauge dynamics which assumed that the soft gauge fields depended only on the direction parallel to the anisotropy vector and time [10]. However, recent numerical studies have now included the transverse dependence of the gauge field and it seems that the result is then that the gauge field's dynamics changes its behavior from exponential to linear growth

---

<sup>1</sup>Soft fields can be thought of as highly occupied low-momentum particle modes. When highly occupied one can ignore the effect of quantum statistics and evolve the fields classically and ensemble average.

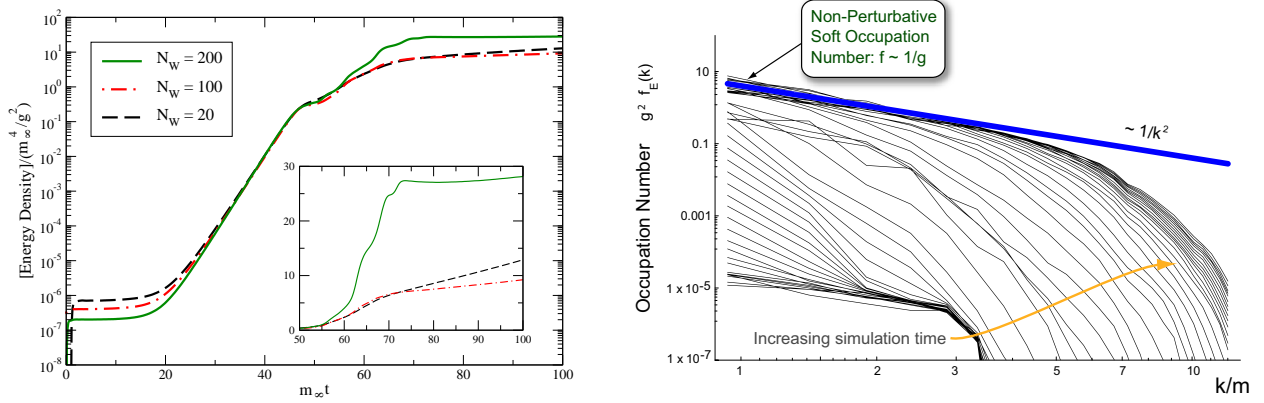


Figure 4: (Left) Comparison of the energy transferred from hard to soft scales by the instability,  $|\mathcal{E}(\text{HL})|$ , for 3+1-dimensional simulations on  $96^3, 88^3, 69^3$  lattices. Inset shows late-time behavior on a linear scale. (Right) Spectrum of modes generated during instability evolution. Early time show clear exponential growth of soft modes followed by “cascade” to a turbulent spectrum with a Kolmogorov scaling of the spectrum  $\sim 1/k^2$ .

when its amplitude reaches the soft scale,  $\langle A \rangle_{\text{soft}} \sim p_{\text{hard}}$  [11, 12]. This linear growth regime is characterized by a cascade of the energy pumped into the soft scale by the instability to higher momentum plasmon-like modes [13] (See Fig. 4 right).

In Fig. 4 (left) I have plotted the time dependence of the energy extracted from the hard particles obtained in a 3+1 dimensional simulation of an anisotropic plasma initialized with very weak random color noise [12]. As can be seen from this figure at  $m_\infty t \sim 60$  there is a change from exponential to linear growth with the late-time linear slope decreasing as  $N_W$  is increased. These results indicate that there is a fundamental difference between abelian and non-abelian plasma instabilities. However, even with this new understanding the HL framework relies on the existence of a large separation between the hard and soft momentum scales by design. One would like to know what happens when the scale separation between hard and soft modes is not very large or when the initial fields have large (non-linear) amplitudes which is seemingly the situation faced in real experiments. In this case one is naturally led to consider instead numerically solving the full non-Abelian Boltzmann-Vlasov equation [14, 15].

### 3.1 Solving the non-Abelian Boltzmann-Vlasov equation

It is also possible to go beyond the hard-loop approximation and solve instead the full classical transport equations in three dimensions [15]. The Boltzmann-Vlasov transport equation for hard gluons with non-abelian color charge  $q^a$  in the are,

$$p^\mu [\partial_\mu - gq^a F_{\mu\nu}^a \partial_p^\nu - gf_{abc} A_\mu^b q^c \partial_{q^a}] f(x, p, q) = \mathcal{C}. \quad (1)$$

Here,  $f(t, \mathbf{x}, \mathbf{p}, \mathbf{q}^a)$  denotes the single-particle phase space distribution function which a function of time, space, momentum, and color charge;  $\mathcal{C}$  denotes hard particle elastic and inelastic collisions.

The Boltzmann-Vlasov equation is coupled self-consistently to the Yang-Mills equation for the soft gluon fields,

$$D_\mu F^{\mu\nu} = J^\nu = g \int \frac{d^3 p}{(2\pi)^3} dq q v^\nu f(t, \mathbf{x}, \mathbf{p}, \mathbf{q}), \quad (2)$$

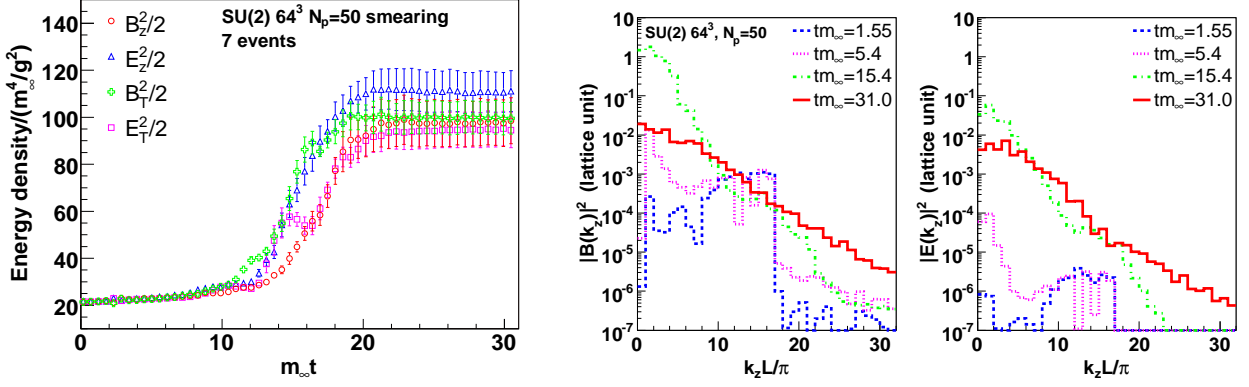


Figure 5: Leftmost figure shows the time evolution of the field energy densities for  $SU(2)$  gauge group resulting from a highly anisotropic initial particle momentum distribution. Simulation parameters are  $L = 5$  fm,  $p_{\text{hard}} = 16$  GeV,  $g^2 n_g = 10/\text{fm}^3$ ,  $m_\infty = 0.1$  GeV. Right two panels show the corresponding fourier transforms of the electric and magnetic fields at different times which are indicated in the legend.

with  $v^\mu \equiv (1, \mathbf{p}/p)$ . These equations reproduce the “hard thermal loop” effective action near equilibrium [18, 19, 20]. However, the full transport theory (1,2) also reproduces some higher  $n$ -point vertices of the dimensionally reduced effective action for static gluons [21] beyond the hard-loop approximation and through the inclusion of collisions goes yet further beyond the hard-loop approximation. The backreaction of the long-wavelength fields on the hard particles (“bending” of their trajectories) is, of course, taken into account, which is important for understanding particle dynamics in strong fields.

Eq. (1) can be solved numerically by replacing the continuous single-particle distribution by a large number of test particles:

$$f(\mathbf{x}, \mathbf{p}, \mathbf{q}) = \frac{1}{N_{\text{test}}} \sum_{\mathbf{i}} \delta(\mathbf{x} - \mathbf{x}_{\mathbf{i}}(t)) (2\pi)^3 \delta(\mathbf{p} - \mathbf{p}_{\mathbf{i}}(t)) \delta(\mathbf{q}^a - \mathbf{q}_{\mathbf{i}}^a(t)), \quad (3)$$

where  $\mathbf{x}_{\mathbf{i}}(t)$ ,  $\mathbf{p}_{\mathbf{i}}(t)$  and  $q_{\mathbf{i}}^a(t)$  are the coordinates of an individual test particle and  $N_{\text{test}}$  denotes the number of test-particles per physical particle. The *Ansatz* (3) leads to Wong’s equations [16, 17]

$$\frac{d\mathbf{x}_{\mathbf{i}}}{dt} = \mathbf{v}_{\mathbf{i}}, \quad (4)$$

$$\frac{d\mathbf{p}_{\mathbf{i}}}{dt} = g q_{\mathbf{i}}^a (\mathbf{E}^a + \mathbf{v}_{\mathbf{i}} \times \mathbf{B}^a), \quad (5)$$

$$\frac{d\mathbf{q}_{\mathbf{i}}}{dt} = ig v_{\mathbf{i}}^\mu [A_\mu, \mathbf{q}_{\mathbf{i}}], \quad (6)$$

$$J^{a\nu} = \frac{g}{N_{\text{test}}} \sum_{\mathbf{i}} q_{\mathbf{i}}^a v_{\mathbf{i}}^\nu \delta(\mathbf{x} - \mathbf{x}_{\mathbf{i}}(t)). \quad (7)$$

for the  $i$ -th test particle. The time evolution of the Yang-Mills field can be followed by the standard Hamiltonian method [22] in  $A^0 = 0$  gauge. For details of the numerical implementation used see Ref. [15].

In Fig. 5 I present the results of the three-dimensional simulations published in Ref. [15]. The leftmost panel shows the time evolution of the field energy densities for  $SU(2)$  gauge group

resulting from a highly anisotropic initial particle momentum distribution. The right two panels show the corresponding fourier transforms of the electric and magnetic fields at different times which are indicated in the legend.

The behavior shown in Fig. 5 indicates that the results obtained from the hard-loop simulations and direct numerical solution of the non-Abelian Boltzmann-Vlasov equations are qualitatively similar in that both show that for non-abelian gauge theories there is a saturation of the energy transferred to the soft modes by the gauge instability. Additionally, as can be seen from the fourier transforms in right two panels of Fig. 5 the saturation is accompanied by an “avalanche” of energy transferred to soft field modes to higher frequency field modes with saturation occurring when the hardest lattice modes are filled. A more thorough analytic understanding of this ultraviolet avalanche is lacking at this point in time although some advances in this regard have been made recently [23]. Additionally, since within the numerical solution of the non-Abelian Boltzmann-Vlasov equations the ultraviolet modes become populated rapidly this means that the effective theory which relies on a separation between hard (particle) and soft (field) scales breaks down. This should motivate research into numerical methods which can be used to “shuffle” field modes to particles when their momentum becomes too large and vice-versa for hard particles. This is a difficult task but work on such algorithms is in progress. Hopefully, using such methods it will be possible to simulate the non-equilibrium dynamics of anisotropic plasmas in a self-consistent numerical framework which treats particles and fields and the transmutation between these two types of degrees of freedom smoothly.

The application of numerical solution of the non-Abelian Boltzmann-Vlasov equations to non-equilibrium QCD is, of course, not limited to the study of anisotropic plasmas. The codes which have been developed by Dumitru, Nara, Schenke, and myself are applicable to study a wide range of real-time response questions, such as jet energy-loss in a dynamic background including the time-evolution of the soft-radiation and radiation/jet back-reaction. These codes will form the basis of a new class of “parton-cascade” codes which don’t have to implicitly rely on assumptions from equilibrium physics, eg. thermal debye screening, to regulate infrared problems encountered in the existing parton cascade codes.

## 4 Hard Thermal Loop Perturbation Theory

At finite-temperature perturbative series for quantities such as the pressure show very poor convergence at temperatures which will be generated during RHIC and/or LHC collisions ( $T/T_c \sim 1-5$ ). One possible conclusion from the problems encountered using conventional finite-temperature perturbation series is that the quark-gluon plasma is completely non-perturbative, and that it can only be studied by non-perturbative methods like lattice gauge theory. This would be a very unfortunate conclusion from the perspective of the search for the quark-gluon plasma. While lattice gauge theory can be used to calculate thermodynamic properties, we have no effective non-perturbative methods for studying the real-time processes that can serve as the signatures for a quark-gluon plasma.

There is another possible interpretation of the failure of the conventional perturbation series. It could simply be a signal that we are using the *wrong degrees of freedom*. Naive perturbation theory is an expansion around an ideal gas of massless quarks and gluons. This generates infrared divergencies that must be cut off either by resumming infinite classes of diagrams or by using non-

perturbative methods. While such a procedure gives a well-defined weak-coupling expansion, the coefficients are too large for the expansion to be of any practical use. It is possible that another choice for the degrees of freedom would generate diagrams with better infrared behavior and a perturbation series with better convergence properties.

The high-temperature limit of QCD provides a clue as to what those degrees of freedom might be. In this limit, quarks and gluons are *quasiparticles* with temperature-dependent masses. Their dispersion relations were first derived by Kalashnikov and Klimov and by Weldon in the early 1980's [30]. Furthermore, quarks and gluons acquire additional propagating degrees of freedom. In addition to the two usual transverse polarization modes of the gluon, there is a collective mode with longitudinal polarization called the plasmon. In addition to the two usual spin states of a quark, there is a collective mode with 2 spin states called the plasmino. The quasiparticle mass of the gluon is also intimately tied to the screening properties of the plasma. Chromoelectric fields are screened by the Debye mechanism beyond a screening length of  $\sim 1/m_g$  where  $m_g$  is the gluon quasiparticle mass. Oscillating chromomagnetic fields are also screened, with a screening length that scales like  $(m_g^2\omega)^{-1/3}$ , where  $\omega$  is the frequency. At very low frequencies  $\omega$  of order  $\alpha_s^2 T$ , non-perturbative effects take over, so that static chromomagnetic fields have a screening length of order  $1/(\alpha_s T)$ .

Quasiparticle masses, collective modes, and screening are all tied together by gauge invariance. The problem is therefore how to incorporate plasma effects into the perturbation expansion for QCD while preserving gauge invariance. This problem was solved at leading order in  $g$  by Braaten and Pisarski [35]. They developed a method called *hard-thermal-loop resummation* for summing all Feynman diagrams that are leading order in  $g$  for amplitudes involving soft external momenta of order  $gT$ . This method can be used to systematically calculate higher order corrections as an expansion in powers of  $g$ . Our method for resumming graphs goes one step beyond normal hard-thermal-loop resummation and I will refer to the general method as *hard-thermal-loop (HTL) perturbation theory* or HTLpt. It is essentially a reorganization of the conventional perturbation expansion for QCD that selectively resums higher order effects related to quasiparticles and screening. The lagrangian for QCD is

$$\mathcal{L}_{\text{QCD}} = -\frac{1}{2}\text{Tr}(G_{\mu\nu}G^{\mu\nu}) + i \sum_{\text{flavors}} \bar{\psi}\gamma^\mu D_\mu\psi. \quad (8)$$

HTL perturbation theory involves adding and subtracting the following *hard-thermal-loop improvement terms*:

$$\mathcal{L}_{\text{HTL}} = -\frac{3}{2}m_g^2 \text{Tr} \left( G_{\mu\alpha} \left\langle \frac{n^\alpha n^\beta}{(n \cdot D)^2} \right\rangle_n G^\mu{}_\beta \right) + im_q^2 \sum_{\text{flavors}} \bar{\psi}\gamma_\alpha \left\langle \frac{n^\alpha}{n \cdot D} \right\rangle_n \psi, \quad (9)$$

where  $n^\alpha = (1, \hat{\mathbf{n}})$  is a light-like four-vector and the angular brackets indicate an average over the direction of  $\hat{\mathbf{n}}$ . Note that the covariant derivatives in the denominators make the HTL improvement terms nonlocal. HTL perturbation theory is the expansion in  $g$  generated by taking the parameters  $m_g^2$  and  $m_q^2$  to be of order 1 in the added  $\mathcal{L}_{\text{HTL}}$  term and of order  $g^2$  in the subtracted  $\mathcal{L}_{\text{HTL}}$  term. The free part of the lagrangian, which consists of the quadratic terms in  $\mathcal{L}_{\text{QCD}} + \mathcal{L}_{\text{HTL}}$ , describes quark and gluon quasiparticles with masses  $m_q$  and  $m_g$ . The corrections due to interactions between the quasiparticles can be systematically taken into account by calculating higher orders in HTL perturbation theory.

One of the attractive features of HTL perturbation theory is that it can be derived directly from QCD. It is essentially a reorganization of the QCD perturbation theory into an expansion around an ideal gas of quasiparticles. Higher order effects related to quasiparticles and screening are summed up into the propagators and vertices of HTL perturbation theory and then systematically subtracted out in higher order diagrams. Observables are calculated in terms of the usual QCD coupling constant  $\alpha_s$  and the quark and gluon mass parameters  $m_q$  and  $m_g$ . But these quasiparticle parameters can be determined as a function of  $\alpha_s$  and  $T$  by the condition that large higher order corrections in the perturbation series be avoided. Thus they are directly related to the fundamental parameter  $\alpha_s$  of QCD.

Another attractive feature is that the HTL perturbation series is gauge-invariant by construction. This follows from the fact that quasiparticle mass parameters  $m_g^2$  and  $m_q^2$  are introduced as coefficients of gauge-invariant terms in the lagrangian, and that perturbation theory is defined as a systematic expansion in a parameter  $g$ . Gauge invariance is useful both as a consistency check in calculations and as a way to simplify calculations.

Calculations in HTL perturbation theory are much more difficult than in ordinary perturbative QCD, because the Feynman rules are more complicated. In spite of the complexity of the Feynman rules, calculations do appear to be tractable. Andersen, Braaten, Petitgirard, and I have demonstrated this by calculating the free-energy to next-to-leading order in HTL perturbation theory [36, 37]. In spite of the complexity of the HTL propagators, we found that the calculation was tractable. There were complicated ultraviolet divergences, but they could be isolated and eliminated using standard renormalization techniques. An analysis of the convergence of the successive approximations obtained using this method shows that we can extend the region of convergence down to  $T/T_c \sim 2-3$  GeV, however, we have found that accessing extremely low temperatures,  $T/T_c < 2-3$  GeV, may not be possible with this method. Despite this apparent failure the method has improved the region of convergence by four orders of magnitude in the temperature in a systematically improvable way which yields completely analytic expressions. I note also that other methods such as the  $\Phi$ -derivable approach have also shown promise for improving the calculation of thermodynamic observables [38]. Together with Jens Andersen I have recently completed the highest-loop-order  $\Phi$ -derivable calculation available for a gauge field theory.

In closing, although the papers written to date have focussed on using HTLpt to compute thermodynamic observables, the true goal of this work is to create a framework which can be applied to both equilibrium and non-equilibrium systems. This will allow a self-consistent determination of both QGP thermodynamics and dynamics. The work outlined in the first section of this statement represents just such an extension of this framework to a non-equilibrium setting. The systematic application of HTLpt to non-equilibrium yields gauge-invariant infrared-safe results for observables which otherwise would be plagued by infrared divergences and gauge variance. This is similar to the advances which were made 15 years ago in equilibrium systems but are now being extended to non-equilibrium systems. The upcoming data coming from RHIC and upcoming LHC runs provides a wealth of new high-precision data on the behavior of nuclear matter under extreme conditions. There will certainly be surprises in the data and the best way to prepare for these surprises is to explore the physics in a systematic theoretical framework based on QCD. The current and forthcoming experimental activity in this field will keep it a lively field of research for years to come.

## References

- [1] A. Dumitru, Y. Nara, B. Schenke and M. Strickland, arXiv:0710.1223 [hep-ph].
- [2] M. Martinez and M. Strickland, arXiv:0709.3576 [hep-ph].
- [3] P. Romatschke and M. Strickland, Phys. Rev. D **69**, 065005 (2004); Phys. Rev. D **71**, 125008 (2005).
- [4] S. M. H. Wong, Phys. Rev. C **54**, 2588 (1996); *ibid.* C **56**, 1075 (1997). R. Baier, A. H. Mueller, D. Schiff and D. T. Son, Phys. Lett. B **502**, 51 (2001); A. H. Mueller, A. I. Shoshi and S. M. H. Wong, arXiv:hep-ph/0505164.
- [5] St. Mrówczyński, Phys. Lett. B **214**, 587 (1988); *ibid.*, Phys. Lett. B **314**, 118 (1993); *ibid.*, Phys. Rev. C **49**, 2191 (1994); *ibid.*, Phys. Lett. B **393**, 26 (1997); St. Mrówczyński and M. H. Thoma, Phys. Rev. D **62**, 036011 (2000).
- [6] P. Romatschke and M. Strickland, Phys. Rev. D **68**, 036004 (2003); *ibid.*, Phys. Rev. D **70**, 116006 (2004).
- [7] P. Arnold, J. Lenaghan and G. D. Moore, JHEP **0308**, 002 (2003).
- [8] St. Mrówczyński, A. Rebhan and M. Strickland, Phys. Rev. D **70**, 025004 (2004).
- [9] P. Arnold and J. Lenaghan, Phys. Rev. D **70**, 114007 (2004).
- [10] A. Rebhan, P. Romatschke and M. Strickland, Phys. Rev. Lett. **94**, 102303 (2005).
- [11] P. Arnold, G. D. Moore and L. G. Yaffe, Phys. Rev. D **72**, 054003 (2005).
- [12] A. Rebhan, P. Romatschke and M. Strickland, JHEP **09**, 041 (2005).
- [13] P. Arnold and G. D. Moore, arXiv:hep-ph/0509206; *ibid.*, arXiv:hep-ph/0509226.
- [14] A. Dumitru and Y. Nara, Phys. Lett. B **621** (2005) 89, hep-ph/0503121.
- [15] A. Dumitru, Y. Nara and M. Strickland, (2006), hep-ph/0604149.
- [16] S.K. Wong, Nuovo Cim. A **65** (1970) 689.
- [17] U.W. Heinz, Phys. Rev. Lett. **51** (1983) 351.
- [18] P.F. Kelly et al., Phys. Rev. Lett. **72** (1994) 3461, hep-ph/9403403.
- [19] P.F. Kelly et al., Phys. Rev. D **50** (1994) 4209, hep-ph/9406285.
- [20] J.P. Blaizot and E. Iancu, Nucl. Phys. B **557** (1999) 183, hep-ph/9903389.
- [21] M. Laine and C. Manuel, Phys. Rev. D **65** (2002) 077902, hep-ph/0111113.
- [22] J. Ambjørn et al., Nucl. Phys. B **353** (1991) 346.
- [23] A.H. Mueller, A.I. Shoshi and S.M.H. Wong, (2006), hep-ph/0607136.
- [24] A.D. Lindé, Phys. Lett. B **96**, 289 (1980).
- [25] P. Arnold and C. Zhai, Phys. Rev. D **50**, 7603 (1994); Phys. Rev. D **51**, 1906 (1995); B. Kastening and C. Zhai, Phys. Rev. D **51**, 7232 (1995).
- [26] E. Braaten and A. Nieto, Phys. Rev. Lett. **76**, 1417 (1996); Phys. Rev. D **53**, 3421 (1996).
- [27] K. Kajantie, M. Laine, K. Rummukainen, and Y. Schroder, Phys. Rev. D **67**, 105008 (2003).
- [28] G. Boyd et al., Phys. Rev. Lett. **75**, 4169 (1995); Nucl. Phys. B **469**, 419 (1996); S. Gottlieb et al., Phys. Rev. D **55**, 6852 (1997); C. Bernard et al., Phys. Rev. D **55**, 6861 (1997); J. Engels et al., Phys. Lett. B **396**, 210 (1997).
- [29] K. Kajantie, K. Rummukainen and M. Shaposhnikov, Nucl. Phys. B **407**, 356 (1993); K. Kajantie, M. Laine, K. Rummukainen and M. Shaposhnikov, Nucl. Phys. B **458**, 90 (1996); K. Kajantie, M. Laine, J. Peisa, A. Rajantie, K. Rummukainen, and M. Shaposhnikov, Phys. Rev. Lett. **79**, 3130 (1997); K. Kajantie, M. Laine, and K. Rummukainen, hep-ph/0007109.
- [30] O.K. Kalashnikov and V.V. Klimov, Sov. J. Nucl. Phys. **31**, 699 (1980); V.V. Klimov, Sov. Phys. JETP **55**, 199 (1982); H.A. Weldon, Phys. Rev. D **26**, 1394 (1982).
- [31] F. Karsch, M.T. Mehr, and H. Satz, Z. Phys. C **37**, 617 (1988); V. Goloviznin and H. Satz, Z. Phys. C **57**, 671 (1993); A. Peshier, B. Kämpfer, O.P. Pavlenko and G. Soff, Phys. Lett. B **337**, 235 (1994); M.I. Gorenstein and S.N. Yang, Phys. Rev. D **52**, 5206 (1995).
- [32] A. Peshier, B. Kämpfer, O.P. Pavlenko, and G. Soff, Phys. Rev. D **54**, 2399 (1996); P. Lévai and U. Heinz, Phys. Rev. C **57**, 1879 (1998).
- [33] F. Karsch, A. Patkós, and P. Petreczky, Phys. Lett. B **401**, 69 (1997).
- [34] J. O. Andersen, E. Braaten and M. Strickland, Phys. Rev. D **63** (2001) 105008; J. O. Andersen and M. Strickland, Phys. Rev. D **64**, 105012 (2001).
- [35] E. Braaten and R.D. Pisarski, Nucl. Phys. B **337**, 569 (1990).

- [36] J. O. Andersen, E. Braaten and M. Strickland, Phys. Rev. Lett. **83**, 2139 (1999); Phys. Rev. D **61**, 014017 (2000).
- [37] J. O. Andersen, E. Braaten, E. Petitgirard and M. Strickland, HTL Perturbation Theory to Two Loops, Phys. Rev. D **66**, 085016 (2002).
- [38] J. P. Blaizot, E. Iancu and A. Rebhan, Phys. Rev. Lett. **83**, 2906 (1999); Phys. Lett. B **470**, 181 (1999); Phys. Rev. D **63**, 065003 (2001).
- [39] J. O. Andersen, E. Petitgirard and M. Strickland, Two-loop Hard-Thermal Perturbation Theory with Quarks, hep-ph/0302069, TUW-03-06, Accepted for publication in Phys. Rev. D, (2003).